

Observational limit on gravitational waves from binary neutron stars in the Galaxy

B. Allen¹, K. Blackburn², P. Brady³, J. Creighton¹, T. Creighton⁴, S. Droz⁵, A. Gillespie², S. Hughes⁴, S. Kawamura², T. Lyons², J. Mason², B.J. Owen⁴, F. Raab², M. Regehr², B. Sathyaprakash⁶, R.L. Savage, Jr.², S. Whitcomb², A. Wiseman¹.

⁽¹⁾*Department of Physics, University of Wisconsin - Milwaukee, PO Box 413, Milwaukee WI 53201.*

⁽²⁾*LIGO Project, MS 18-34, California Institute of Technology, Pasadena, CA 91125.*

⁽³⁾*Institute for Theoretical Physics, University of California, Santa Barbara, CA 93106*

⁽⁴⁾*Theoretical Astrophysics 130-33, California Institute of Technology, Pasadena, CA 91125.*

⁽⁵⁾*Department of Physics, University of Guelph, Guelph, ON N1G 2W1, Canada.*

⁽⁶⁾*Department of Physics and Astronomy, UWCC, Post Box 913, Cardiff CF2 3YB, Wales.*

We analyze 25 hours of data from the LIGO 40-meter prototype laser interferometric gravitational wave detector taken during the third week of November 1994. The instrument was sensitive enough to detect the gravitational-wave chirps that would be emitted by coalescing compact binary systems within our Galaxy. The data stream was searched using optimal matched filtering — the first implementation/test of this technique on real interferometric data. These methods will be an important part of upcoming LIGO data analysis. An upper limit on the rate R of neutron star binary inspirals in our Galaxy is obtained: with 90% confidence, $R < 0.5/\text{hour}$. Similar experiments with LIGO interferometers will provide constraints on the population of tight binary neutron star systems in the Universe.

A world-wide effort is underway to construct and operate a new generation of broad-band gravitational radiation detectors. These include the US Laser Interferometer Gravitational-wave Observatory (LIGO) [1] project, the French/Italian VIRGO project [2], the British/German GEO-600 project [3], the Japanese TAMA project [4], and the Australian ACIGA project [5]. The detectors are laser interferometers containing suspended optical elements: a gravitational wave changes the relative optical phase in two perpendicular paths, shifting the interference pattern at the beam splitter [6]. Within the next decade, these facilities should permit direct experimental observation of gravitational waves from sources at tens to hundreds of Mpc distance.

A 40-meter interferometer has been under development at Caltech since 1983. During the past decade, the LIGO project has used this prototype instrument to develop and test the optical and control elements for the full scale detectors under construction in Hanford WA and Livingston LA [7]. In November 1994, this instrument was configured as a suspended, modulated Fabry-Perot interferometer: light returning from the two arms was independently sensed [8]. In this configuration, the detector had its best differential displacement sensitivity of $\approx 3.5 \times 10^{-19} \text{ m Hz}^{-1/2}$ over a bandwidth of approximately a kHz centered at 600 Hz.

A week-long test run of the instrument was made between 14 and 20 November 1994 prior to a major reconfiguration. This run yielded 44.8 hours of tape; both arms were in optical resonance for 39.9 hours (89% of the time). The data-taking periods are shown in Fig. 1. Although the November 1994 data was taken for diagnostic purposes, it provides an excellent opportunity to extract observational limits on gravitational wave sources, and to examine analysis techniques.

A major challenge arises because the real data stream does not satisfy the usual stationary and Gaussian assumptions. The 40-m data have the expected colored broadband background but with significant deterministic components (spectral peaks); these include $\sim 10^2$ sinusoidal components arising from mechanical modes of the suspension and 60 Hz line

harmonics. There are also transient features occurring every few minutes: bursts of noise with durations between ~ 1 and ~ 500 ms. Burst sources include accidental excitation of high-order transverse optical modes driven by (natural or man-made) seismic disturbances, strain releases in mechanical structures, saturation of electronic servo loops, and EMI. These deviations from Gaussian noise are extremely difficult to model and classify using standard techniques. This led us to develop filter approximations and time/frequency statistical tests which make matched filtering methods perform well on real data.

This Letter reports the techniques, details, and results of a search through this data set for binary inspiral chirps—the gravitational waveforms produced by pairs of orbiting compact stars or black holes. For concreteness, we focus our attention on neutron star binaries in our Galaxy. These systems emit gravitational waves (primarily at twice the orbital frequency) over periods of tens to hundreds of millions of years, gradually losing energy. As the stars move closer together, the orbit circularizes and its period decreases. The search reported here is for the gravitational waves that would be emitted during the final few seconds of this process; the stars orbit hundreds of times per second at separations of tens of km before plunging together. Preliminary searches performed using 40-meter data are reported in Refs. [7,9].

The data stream was searched using *matched filtering*. This method [10] uses linear filters constructed from the expected waveforms. These waveforms have been calculated by two independent groups (with identical results) in the 2nd-order post-Newtonian (2PN) approximation, using different techniques [11]. Careful estimates suggest that these approximations result in a reduction of $\leq 10\%$ of signal to noise ratio (SNR) [12]. For example, the waveform for a $2 \times 1.4 M_{\odot}$ binary is a sweeping sinusoid which enters the pass band of the detector around 120 Hz. The frequency and amplitude increase during the ensuing 255 cycles; after 1.35 seconds the frequency has increased to 1822 Hz and the waveform is cut off by the merger of the stars.

gr-qc/9903108 31 Mar 1999

The effect of the gravitational wave on the detector is described by a dimensionless strain $h(t)$. The gravitational wave produces a differential change $\Delta L(t) = Lh(t)$ in the lengths of the two perpendicular interferometer arms [6], where $L = 38.25\text{m}$ is the average arm length. For a binary system (circular orbits, no spin) with masses $M = (m_1, m_2)$ this strain is:

$$h(t) = \frac{1 \text{ Mpc}}{D} [\sin \alpha h_s^M(t - t_0) + \cos \alpha h_c^M(t - t_0)].$$

Here α is a constant determined by the orbital phase and orientation of the binary system, t_0 is the laboratory time at which the chirp signal first enters the detector pass-band, and $h_{s,c}^M(t - t_0)$ are the amplitudes of the two polarizations of the gravitational waveform produced by an inspiraling binary system which is optimally oriented at 1 Mpc. An optimally oriented binary system would be located on the z -axis of a coordinate system in which the two interferometer arms define the x, y -axes, and with the normal to its orbital plane parallel to the z -axis. The effective distance D depends on the distance to the source and on its orientation with respect to the detector, which has a non-uniform response. If the source is not optimally oriented, then D is greater than the source-detector distance. The 2PN formulae for $h_{s,c}^M$ are taken from [11].

Our primary detector signal is derived from the feedback forces applied to hold the interferometer in resonance. This signal, which is proportional to the differential-displacement $\Delta L(t)$, is filtered to increase the dynamic range of the recording system by attenuating the large seismically driven, low-frequency components of the detector output, and to prevent aliasing by attenuating the high frequencies. This filtered voltage $v(t)$ was recorded at a 9868.42 Hz sample rate by a 12 bit analog-to-digital converter. The reduction of SNR arising from quantization errors is less than 0.9% [13]. The instrument's frequency and phase response $\tilde{R}(f)$ was determined at the beginning of each of eleven ~ 4 hour data runs using a swept-sine calibration [14] in which known perturbative forces were applied to the interferometer. The eleven calibration curves differ by less than 5%, having the largest variations around the 1 kHz unity-gain point of the differential-mode servo loop. Because errors in calibration affect the SNR only at second order, we estimate the effects of any calibration errors or drifts on SNR to be less than 0.3%. The voltage output $v_h(t)$ that would be produced by a binary inspiral is given by

$$v_h(t) = \int_{-\infty}^t R(t-t')h(t')dt' = \int_{-\infty}^{\infty} \tilde{h}(f)\tilde{R}^*(f)e^{-2\pi ift}df$$

using the notation $Q(t)$ and $\tilde{Q}(f)$ to denote Fourier-transform pairs.

We search for inspiral waveforms using (digital) matched filtering. Because the inspiral waveforms depend upon the source masses $M = (m_1, m_2)$ we use a "bank" of template waveforms placed closely enough [15] in parameter space to detect any signal in the mass range $1.0 M_\odot < m_1, m_2 <$

$3.0 M_\odot$ [16]. The bank contains 687 filters M_k and is designed so that no more than 2% of SNR would be lost if the mass parameters M of a signal did not exactly match one of the M_k . For each mass pair M_k in the template bank two real signals are constructed:

$$X_k^{s,c}(t) = N_k^{s,c} \int_{-\infty}^{\infty} \frac{\tilde{v}(f)\tilde{h}_{s,c}^{*M_k}\tilde{R}(f)}{S_v(|f|)}e^{-2\pi ift}df. \quad (1)$$

These are the time-domain outputs of optimal filters matched to the waveform of the k th mass-pair M_k . The denominator $S_v(|f|)$ is (an estimate of) the one-sided power spectral density of $v(t)$; if the detector's noise is stationary and Gaussian, then these filters are optimal. The normalization factor $N_k^{s,c}$ is chosen so that, in the absence of any signals, the mean value of $[X_k^{s,c}(t)]^2$ is unity. We define the SNR for the k th template waveform to be

$$\rho_k(t) = \text{SNR} = \sqrt{[X_k^s(t)]^2 + [X_k^c(t)]^2},$$

arrived at by maximizing over the phase α of the binary system. The effective distance D at which coalescence of $2 \times 1.4 M_\odot$ stars would yield an SNR of 10 in the interferometer is shown in Fig. 1. (The normalization of the SNR follows Ref. [15] and other literature on data analysis. The root-mean-square value of the SNR for a single template is $\sqrt{2}$ in the presence of Gaussian noise alone.)

The data was processed, using FFT methods, in overlapping ≈ 26.6 s segments (2^{18} samples). To avoid end effects, $S_v^{-1}(|f|)$ in Eq. (1) was truncated at ≈ 13.3 s in the time domain. The longest chirp signal was ≈ 2.4 s long, so the data were overlapped by the total filter impulse response time of ≈ 15.6 s (155 072 samples) giving a filter output duration of ≈ 10.85 s/segment. Since the process of bringing the optical cavities into resonance (lock) excites mechanical modes of the suspension wires, we discarded the first three minutes of data after each lock acquisition, allowing the mechanical modes to damp below other noise sources. Of the 39.9 locked hours of data, 8.8 hours were in intervals too short to analyze; 111 locked intervals remained. Discarding the startup transient impulse response of the filters and the first three minutes of lock yielded $39.9 - 8.8 - 6.0 = 25.0$ hours of data analyzed, in 8289 intervals of filter output (Fig. 1).

The data are corrupted by sources of non-stationary noise that are poorly understood. Because of the broad-band nature of the interferometric detector, one can reject many of these transient events; they do not have the time-frequency behavior of the chirp signals we are searching for. In our search, these transient events are discriminated from chirps by a χ^2 time-frequency test (Sec. 5.24 of Ref. [16]). The frequency band (DC to Nyquist) is divided into p subintervals, chosen so that for a chirp superposed on Gaussian noise with the observed power spectrum the expected contribution to ρ is equal for each subinterval. One then forms a statistic χ^2 by summing the squares of the deviations of the p signal values from the expected value for each of the two template polarizations. We

choose $p = 20$ so that Galactic signals which fall at the maximal template mismatch would not be rejected. In the presence of Gaussian noise plus chirp the statistic has a χ^2 distribution with $2p - 2 = 38$ degrees of freedom [16].

Occasionally, there are glitches in the data when the instrument's output significantly exceeds its RMS value. Some of these arise from seismically-induced mode-cleaner rocking, which excites off-axis optical modes. These glitches cause the outputs of the optimal filters to ring, but do not resemble binary inspiral chirps and are uniformly rejected by the time-frequency technique described above. However these glitches bias $S_v(|f|)$ enough to create non-optimal filters. To prevent this problem the power spectrum was estimated by averaging it for the 8 glitch-free segments closest in time to the segment being analyzed. The glitches were identified by seeing if too many samples fell outside a $\pm 3\sigma$ range or any fell outside a $\pm 5\sigma$ range. The number of segments (8) was chosen to reduce the variance of the spectrum while still tracking changes in instrument performance.

About 32 hours of clock time on a 48 node DEC Alpha based Beowulf computer system at UWM were required to process this data. Each node has a theoretical peak performance of 600 double-precision Mflops; the maximum throughput is 29 GFlops. The output of the filtering process is a list of signals for each segment j : the maximum (over t) SNR obtained for each filter k in our bank of 687 filters, the time t_j at which that maximum occurred, the value of the χ^2 statistic for that filter, and $N^{s,c}$. In a given segment of data, we say that an event has occurred if the maximum SNR, over all filters for which the statistic χ^2 lies below some threshold χ_*^2 , exceeds a threshold ρ_* . The total number N of events observed in the data set of Fig. 1 is plotted as a function of these thresholds in Fig. 2.

Without operating two or more detectors in coincidence, it is impossible to characterize the non-Gaussian and non-stationary background well enough to establish confident detection. However one may estimate upper limits on the rate of Galactic neutron star binary inspirals (Poisson-distributed in time) using a method which requires minimal assumptions about detector noise. Our limit $R_{90\%}$ is based on the probability of a Galactic neutron star binary signal being as loud (having a SNR as large) as the loudest observed event. If the rate is greater than $R_{90\%}$ then it is likely that we would observe louder events. Because the detector was only sensitive to a fraction of Galactic binary inspirals (Fig. 1), the event-rate bound depends on two numbers: (i) the efficiency ϵ_{\max} with which the instrument and filtering/analysis process can detect a binary inspiral in the Galaxy at the SNR ρ_{\max} of the loudest observed event, and (ii) the total length $T = 25.0$ hours of filtered data.

We determined the efficiency ϵ by Monte-Carlo simulation, doing additional runs through the data set, and adding simulated Galactic inspiral waveforms [convolved with the detector response function $\tilde{R}(f)$] at 30 s intervals into the detector output $v(t)$. *This allows us to characterize the detection process with the properties of the real instrumental noise rather*

than an ad-hoc model. The injected waveforms were drawn from a population of binary neutron stars with a spatial number distribution given by $dN \propto e^{-D^2/2D_0^2} D dD \times e^{-|Z|/h_Z} dZ$ where D is Galactocentric radius, $D_0 = 4.8$ kpc, Z is height off the Galactic plane, and $h_Z = 1$ kpc is the scale height. This distribution is similar to the one presented in Ref. [17]. The detection efficiency ϵ is the fraction of these simulated inspirals which registered as events in our filtering/analysis procedure; it increases as the SNR threshold ρ_* is decreased, or as χ_*^2 is increased, and is shown in Fig. 2 for the most-probable mass range [18] of 1.29 to 1.45 M_\odot (the results depend very weakly on the mass).

The results of our analysis give an event rate bound. With 90% confidence, the rate of binary inspirals in our Galaxy is less than $R_{90\%} = 3.89/[T\epsilon(\rho_{\max}, \chi_*^2)]$ where ρ_{\max} is the largest SNR event observed, and the threshold $\chi_*^2 = 49.5$ is chosen so that there is a 10% chance of rejecting a real chirp signal in stationary Gaussian noise. (This is a Bayesian credible interval computed using a "uniform prior" for the event rate. The dimensionless numerator depends only on the confidence level.) Thus we find $\rho_{\max} = 8.34$ at $\chi_*^2 = 49.5$. The efficiency $\epsilon_{\max} = 0.33$ gives $R_{90\%} = 0.5/\text{hour}$. This is a 90% confidence limit if the loudest event is a real binary inspiral event. If the loudest event is noise, the confidence is $\geq 90\%$. Thus, $R_{90\%}$ gives a conservative upper limit on the event rate when the detector noise is poorly understood. (While some of the louder events in Fig. 2 are instrumental artifacts arising from seismic disturbances or laser power fluctuations, the loudest event was detected during fairly normal instrument operation.)

It is useful to compare the limit obtained here, $R_{90\%} = 0.5/\text{hour}$, with the limit that could be obtained from the ideal analysis of an instrument that could detect every Galactic event. Operating for the same total time $T = 25.0$ hours with an efficiency $\epsilon = 1$, the limit obtained would be three times better: $R_{90\%} = 0.17/\text{hour}$.

Stellar population studies [19] indicate expected rates $R \sim 10^{-6}\text{yr}^{-1}$, far below our limit. Nevertheless this work does provide a direct observational limit on these rates from a new type of search, and it demonstrates some of the methods being developed to analyze data from the next generation of instruments. A previous search using 100 hours of coincident Glasgow/Garching interferometer data gave an upper limit on burst sources [20]. The current generation of resonant-mass detectors [21] has established upper limits on monochromatic signals and stochastic background, but not on binary inspiral. A coincidence analysis of bar data for coalescing binaries might produce a stronger limit than ours; these bars are sensitive enough to detect coalescing binaries throughout the Galaxy and have accumulated much more observation time.

The LIGO interferometers will permit detailed analysis impossible to achieve with the prototype experiment. Comprehensive instrument monitoring will permit the thorough characterization of instrument anomalies and removal of some environmental noise. Simultaneous correlation between three

independent instruments will provide lower false alarm rates and greater statistical confidence. This will augment the techniques used here and allow LIGO to detect sources, as well as set tight rate limits. For example, if the loudest coincident event detected by the LIGO interferometers has a SNR $\rho_{\max} = 5.5$, then we would obtain the limit

$$\mathcal{R}_{90\%} = 6 \times 10^{-5} \text{Mpc}^{-3} \text{yr}^{-1} \left(\frac{55 \text{Mpc}}{r_{\max}} \right)^3 \left(\frac{1 \text{yr}}{T_{\text{obs}}} \right),$$

on the rate of inspiral in the universe, where T_{obs} is the observation time, and r_{\max} is the distance to an optimally oriented source with SNR $\rho_{\max} = 5.5$. For the initial LIGO interferometers, the distance is $r_{\max} = 55 \text{Mpc}$; it will be ten times larger for the enhanced interferometers, giving an expected rate limit of $6 \times 10^{-8} \text{Mpc}^{-3} \text{yr}^{-1}$. These limits should be compared to the best guess rate of $8 \times 10^{-8} \text{Mpc}^{-3} \text{yr}^{-1}$ given by Phinney [19].

This work was supported by National Science Foundation grants PHY9210038, PHY9407194, PHY9424337, PHY9507740, PHY9603177, and PHY9728704. P.R.B. is grateful to the Sherman Fairchild foundation for financial support. J.C. was supported in part by NSERC of Canada. B.A. acknowledges the kind efforts of the LIGO project in making its data and resources available for our use, and thanks B. Mours and his VIRGO colleagues for their assistance.

[1] A. Abramovici *et al.*, *Science* **256**, 325 (1992).
[2] B. Caron *et al.*, in *Gravitational Wave Experiments*, edited by E. Coccia, G. Pizzella, and F. Ronga, (World Scientific, Singapore, 1995).
[3] K. Danzmann *et al.*, in *Gravitational Wave Experiments*, edited by E. Coccia, G. Pizzella, and F. Ronga, (World Scientific, Singapore, 1995).
[4] K. Tsubono, in *Gravitational Wave Experiments*, edited by E. Coccia, G. Pizzella, and F. Ronga, (World Scientific, Singapore, 1995).
[5] R. John Sandeman, in *Second workshop on gravitational wave data analysis*, edited by M. Davier and P. Hello, Éditions Frontières, Paris, 1998).
[6] P. R. Saulson, *Fundamentals of interferometric gravitational wave detectors*, (World Scientific, Singapore, 1994).
[7] T. T. Lyons, Ph.D. thesis, Caltech, 1997; A. D. Gillespie, Ph.D. thesis, Caltech 1995.
[8] A. Abramovici *et al.*, *Phys. Lett. A* **218**, 157 (1996).
[9] S. Smith, Ph.D. thesis, Caltech, 1988.
[10] C. Cutler and É. É. Flanagan, *Phys. Rev. D* **49**, 2658 (1994); R. Balasubramanian, B. S. Sathyaprakash, and S. V. Dhurandhar, *ibid.* **53**, 3033 (1996); Erratum *ibid.* **54**, 1860 (1996).
[11] L. Blanchet, B. R. Iyer, C. M. Will, and A. G. Wiseman, *Class. Quantum Grav.* **13**, 575 (1996); C. M. Will and A. G. Wiseman, *Phys. Rev. D* **54**, 4813 (1996); L. Blanchet, T. Damour, B. R. Iyer, C. M. Will, and A. G. Wiseman, *Phys. Rev. Lett.* **74**, 3515 (1995).
[12] S. Droz and E. Poisson, Sec. 6 in Ref. [16]; S. Droz, *Phys. Rev. D* **59**, 064030 (1999).
[13] B. Allen and P. Brady, Report No. LIGO-T970128-01-E, 1997 (unpublished).
[14] Robert Spero, Report No. LIGO-T970232-00-R, 1997 (unpublished).

[15] B. J. Owen, *Phys. Rev. D* **53**, 6749 (1996).
[16] B. Allen *et al.*, *GRASP: a data analysis package for gravitational wave detection* version 1.8.4. Manual and package at: <http://www.lsc-group.phys.uwm.edu/>.
[17] S. J. Curran and D. R. Lorimer, *Mon. Not. R. Astron. Soc.* **276**, 347 (1995).
[18] L. S. Finn, *Phys. Rev. Lett.* **73**, 1878 (1994).
[19] E. S. Phinney, *Astrophys. J.* **380**, L17 (1991).
[20] D. Nicholson *et al.*, *Phys. Lett. A* **218**, 175 (1996).
[21] P. Astone *et al.*, *Astropart. Phys.* **7**, 231 (1997); P. Astone *et al.*, *Phys. Lett. B* **385**, 421 (1996); E. Maucelli *et al.*, *Phys. Rev. D* **56**, 6081 (1997).

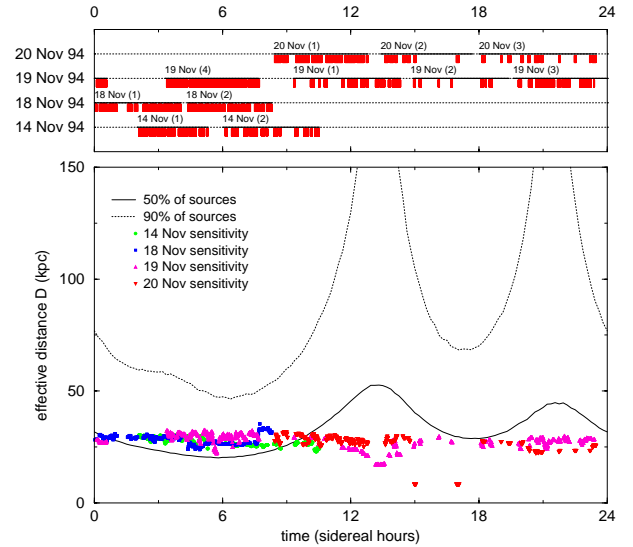


FIG. 1. Eleven data runs (and filtered intervals) from November 1994 are shown as functions of sidereal time in the upper plot. The effective distance D at which inspiral of $2 \times 1.4M_{\odot}$ stars would produce an SNR $\rho = 10$ in the instrument is shown below; also shown is the time variation of D to 50% (solid) and 90% (dotted) of binary sources as the detector's beam pattern swings by the Galactic bulge.

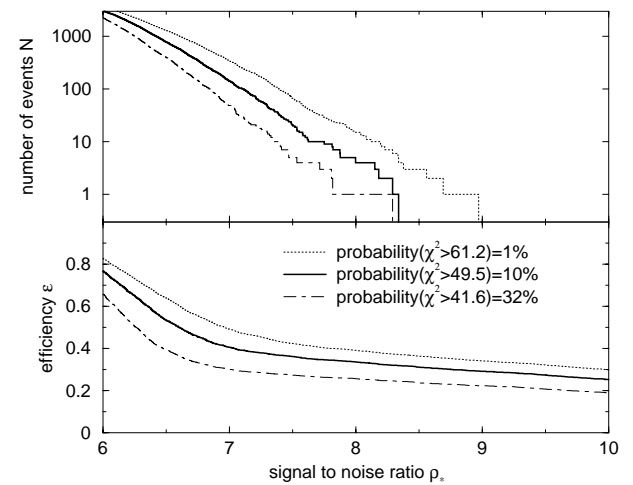


FIG. 2. Top: total number N of events observed, as a function of the SNR threshold ρ_* and the threshold χ_*^2 . Bottom: fraction ϵ of Galactic inspiral chirp signals that would lie above the SNR threshold ρ_* and below the threshold χ_*^2 .

Note 1, LIGO, 04/05/99 10:03:17 AM
LIGO-P990019-00-E